Biol. Cybern. 83, 517–527 (2000)

Biological Cybernetics

Mechanical models for insect locomotion: dynamics and stability in the horizontal plane – II. Application

John Schmitt[1], **Philip Holmes**[1,2]

[1] Department of Mechanical and Aerospace Engineering, Princeton University, Princeton, NJ 08544, USA
[2] Program in Applied and Computational Mathematics, Princeton University, Princeton, NJ 08544, USA

Received: 6 September 1999 / Accepted in revised form: 8 May 2000

Abstract. We study the dynamics and stability of legged locomotion in the horizontal plane. We discuss the relevance of idealized mechanical models, developed in a companion paper, to recent experiments and simulations on insect running and turning. Applying our results to rapidly running cockroaches, we show that the models' gait and force characteristics match observations reasonably well.

1 Introduction: insect locomotion

In this paper, we apply the simple bipedal mechanical models for legged locomotion developed in the preceeding paper (Schmitt and Holmes 2000a) to rapidly running cockroaches. We describe the results of simulations illustrating the analyses of Schmitt and Holmes (2000a), and compare them with experiments of Full et al. (Full and Tu 1990, 1991; Ting et al. 1994), simulations by Kubow and Full of a rigid body subject to prescribed hexapedal foot forces based on forces observed in such experiments (Kubow and Full 1999), and to observations on turning behavior due to Jindrich and Full (1999).

We recall the basic equations of motion in the inertial frame from Schmitt and Holmes (1999):

$$m\ddot{\mathbf{r}} = \mathbf{R}(\theta(t))\mathbf{f}, \quad I\ddot{\theta} = (\mathbf{r}_F - \mathbf{r}) \times \mathbf{R}(\theta(t))\mathbf{f} \ . \tag{1}$$

Here, $\mathbf{r}$ denotes mass center (COM) position, θ body orientation, $\mathbf{R}(\theta)$ is the rotation matrix, and $\mathbf{r}_F$ is the foot position at touchdown, computed as described by Schmitt and Holmes (2000a) and remaining fixed during each stride. A 50% duty cycle is assumed. The foot force $\mathbf{f}$ is supposed to act along the leg, and is either specified externally [prescribed force model], or derived from the displacement of a passive elastic leg [compliant fixed and moving center of pressure (COP) and prescribed leg angle models]. For the latter models, it is convenient to use polar coordinates during each stance phase, in terms of which the Hamiltonian equations of motion become, for the linear spring case

$$\begin{aligned}
\dot{\zeta} &= \frac{p_\zeta}{m}, \quad \dot{p_\zeta} = \frac{p_\psi^2}{m\zeta^3} - \frac{k(\eta - l_0)}{\eta}\{\zeta + d\sin[\psi - (-1)^n\theta]\} \\
\dot{\psi} &= \frac{p_\psi}{m\zeta^2}, \quad \dot{p_\psi} = -\frac{k(\eta - l_0)}{\eta} d\zeta\cos[\psi - (-1)^n\theta] \\
\dot{\theta} &= \frac{p_\theta}{I}, \quad \dot{p_\theta} = (-1)^n\ \frac{k(\eta - l_0)}{\eta} d\zeta\cos[\psi - (-1)^n\theta] \ ,
\end{aligned} \tag{2}$$

for fixed COP. For the moving COP model of Schmitt and Holmes (2000a), with $d = d_0 + d_1[\psi - (-1)^n\theta]$, one adds $-d_1k(1 - l_0/\eta)\{d + \zeta\sin[\psi - (-1)^n\theta]\}$ and $+d_1k(1 - l_0/\eta)\{d + \zeta\sin[\psi - (-1)^n\theta]\}$, respectively, to the fourth and sixth components of (2). The three degrees of freedom (ζ, ψ, θ) describe COM positions relative to the 'active' foot and body orientation, and $\eta = \sqrt{\zeta^2 + d^2 + 2\zeta d\sin(\psi - \theta)}$ denotes the (compressed) leg length. The integer n counts stance phases, using the convention n even for left (L) and n odd for right (R). The model is characterized by six physical parameters: body mass, m, and moment of inertia, I; leg stiffness, k, and relaxed leg length, l_0; pivot position (COP) relative to COM, d; leg touchdown angle β. Defining nondimensional time $\tilde{t}$, these reduce to four nondimensional groups:

$$\tilde{k} = \frac{kl_0^2}{mv^2}, \quad \tilde{I} = \frac{I}{ml_0^2}, \quad \tilde{d} = \frac{d}{l_0}, \quad \beta; \quad \text{with } \tilde{t} = \frac{v_0 t}{l_0} \ , \tag{3}$$

where v is a characteristic COM velocity. For moving COP, $\tilde{d}$ is replaced by $\tilde{d}_j = d_j/l_0;\ j = 0, 1$.

In Schmitt and Holmes (2000a), it is shown that these models exhibit periodic gaits for a range of forward speeds above a critical speed (or, equivalently, below a critical $\tilde{k}$ depending on β), at which a saddle-node bifurcation occurs. The 'physical' branch of gaits

Correspondence to: P. Holmes

emanating from this is asymptotically stable with respect to heading and body angular velocity, provided $d < 0$ (or $d_1 < 0$, for moving COP).

2 Simulations of rapidly running cockroaches

The following simulations were done in Matlab, using Runge-Kutta integration of the equations of motion in both inertial and polar coordinates, with indistinguishable results. Parameters were set to values typical for the death-head cockroach *Blaberus discoidalis* (Ting et al. 1994; Kram et al. 1997; Kubow and Full 1999): $m = 0.0025$ kg, $I = 2.04 \times 10^{-7}$ kg m^2, $k = 0.5 - 3.5$ N m^{-1}. Spring constants were chosen to match peak forces characteristic of steady running at 0.2–0.25 m s^{-1} with reasonable leg compressions ($\leq$50%). We considered various touchdown angles and leg lengths: $\beta = \pi/4$, $l_0 = 0.017$ m, leads to long strides and slow leg cycle rates around 4–5 Hz at forward speeds in the 0.2–0.25-m s^{-1} range; increasing β to 1 gives rates of 6–8 Hz; finally, decreasing l_0 to 0.01 m with $\beta = 1$ gives stride lengths and cycle rates of about 10 Hz, close to those observed in the animal. For these parameter values, the velocities for which $\tilde{k} = 1$ lie above 0.25 m s^{-1}, so the following simulations are within the regime for which the linear spring model is reasonable (see the remarks following (33) in Sect. 3.2 of Schmitt and Holmes 2000a).

Further parameter studies will be described elsewhere (Schmitt and Holmes 2000b; Schmitt et al. 2000), but in passing we observe that both the fixed and moving COP models display constant stride lengths with increasing forward speed. One may even give explicit formulae based on simple geometrical constructions appealing to L-R reflective symmetry (see the diagram in Fig. 2a). We have

$$L_s = 4l_0 \cos\beta \text{ and}$$
$$L_s = 4[\bar{d}\cos\beta + l_0\cos(\beta + \bar{\theta})] \approx 4(l_0 + \bar{d})\cos\beta \ , \qquad (4)$$

(for small $|\bar{\theta}|$), respectively, where $\bar{d}$ and $\bar{\theta}$ are the maximal excursion of COP from COM and body angle magnitude at touchdown in the moving COP (latter) case. This assists in parameter choices, and also agrees with the experimental observation that stride length is approximately constant in the range 0.05–0.30 m s^{-1}; see Ting et al. (1994) and Fig. 2.

2.1 Running with fixed center of pressure

We first consider gaits of the compliant-legged, free pivot biped of Sect. 3.1–3.3 of Schmitt and Holmes (2000a). Simulations of running were carried out for $d < 0$, $d = 0$, and $d > 0$. The results of Fig. 1, with $k = 0.53$, $l_0 = 0.017$, $\beta = \pi/4$, corroborate the stability calculations presented in Sect. 3.2–3.3 of Schmitt and Holmes (2000a). For $d < 0$, starting from an arbitrary initial state with mass center and angular velocities and body orientation not at gait equilibrium values, the motion meanders briefly before settling to a stable gait with small oscillations about a constant angle θ. For $d = 0$, similar behavior ensues, provided the initial angular velocity is zero. For $d > 0$, however, a stable gait is not achieved; the center of mass diverges and

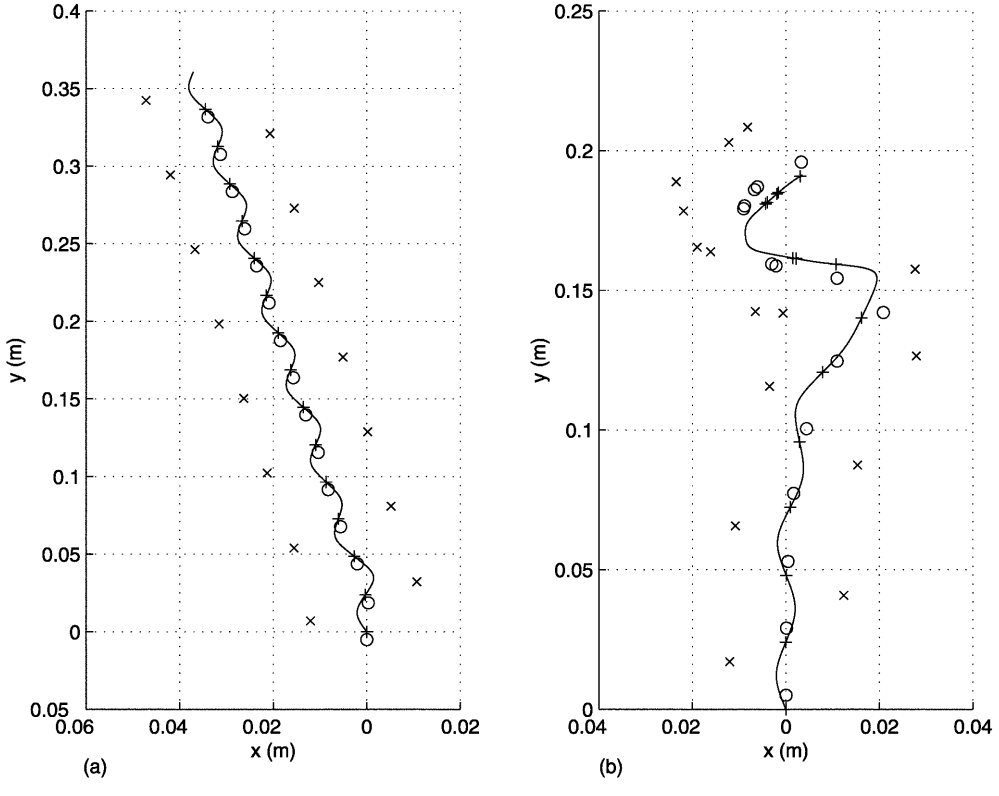

Fig. 1. Stable (**a**) and unstable (**b**) motions of the elastic legged system with $d = -0.005$ and $+0.005$, respectively. Other parameter values given in text. $\times$'s represent foot positions, o's and $+$'s, positions of leg attachment point P and mass center G at touchdown/liftoff

zigzags and ultimately the body 'bounces back' and foot placements collide.

For the $d = 0$ case, we use a modified Newton-Raphson iteration coupled with Runge-Kutta numerical integration of (2) to find a periodic gait and its associated eigenvalues. A sample fixed point thus found is: $\bar{v} = 0.3$, $\bar{\delta} = 0.09852$, $\bar{\theta} = 0$, and $\dot{\theta} = 0$, with the single non-unity eigenvalue 0.2421. The analytical map of Schmitt and Holmes (2000a), Sect. 3.2, using the elliptic function quadratures computed there for the same fixed point values, delivers 0.2416, a difference of only 0.2%. In general, the values $(v_{n+1}, \delta_{n+1}, \theta_{n+1})$ obtained by simulating for one stride, agreed within 1.0% with those predicted by the map. These comparisons provide checks of our numerical calculations.

We now examine the character of steady gaits. Comparing forward and lateral velocities during the stride to those reported by Full and Tu (1990) and Kram et al. (1997) and reproduced in the model of Kubow and Full (1999), reveals that they match reasonably closely those observed for the cockroach (Fig. 2b). Forces generated at the foot (or equivalently, at P) also compare fairly well both in orders of magnitude and time histories to those for summed leg tripods (Fig. 2c), although the peak fore-aft forces (± 0.0014 N) and lateral forces (± 0.0041 N) have magnitudes 'reversed' from ± 0.004 N and ± 0.0032 N taken in Kubow and Full (1999). However, θ variation for the model differs markedly from observations; it approximates a negative sinusoid (third panel of Fig. 2b). This is due to the torque, which is positive during L-stance and negative during R-stance, since $d < 0$ (third panel of Fig. 2c). Experimental studies (Kram et al. 1997) reveal that θ behaves more like a positive cosinusoid, with $\dot{\theta} \approx 0$ at touchdown and liftoff. Note that our velocities and force components are referred to inertial coordinates, but that since θ remains small, they approximately coincide with body coordinates.

A steady gait was also found for $\beta = 1.0$; here the velocity and angle oscillations ($\dot{y} = 0.21 \pm 0.02$ m s^{-1}, $\dot{x} = \pm 0.02$ m s^{-1}, $\theta = \pm 0.035$ rad s^{-1}), and peak fore-aft and lateral forces (± 0.0004 N, ± 0.0018 N) were considerably smaller than those observed, although the temporal frequency of 5.9 Hz was closer to that in the animal at this forward speed. Decreasing l_0 to 0.1 and increasing k to 2.25 (to keep $\tilde{k}$ approximately constant at preferred speed) gives a gait with the appropriate 10 Hz frequency at 0.22 m s^{-1}, and with peak fore-aft and lateral forces of ± 0.0011 N and ± 0.0047 N and correspondingly smaller fore-aft velocity and body angle variations (less than $\pm 1°$), due to reduced integrated force and torque impulses resulting from the shorter stride duration. The fact that fore-aft forces are always smaller than lateral forces in the model is due to our single leg and 'in-line' force vector (Schmitt and Holmes 2000b).

Following the lead of Kubow and Full (1999), we next examine the effects of perturbating forward, lateral and angular velocities of a stable ($d < 0$) gait from their nominal values (here 0.218 m s^{-1}, -0.0547 m s^{-1} and -3.30 rad s^{-1}, respectively; see Fig. 3). Perturbations of ± 0.01 m s^{-1} and ± 0.02 m s^{-1} in forward and lateral velocities and ± 0.3 rad s^{-1} and ± 0.6 rad s^{-1} in angular velocity, were applied as discontinuous jumps directly after touchdown. In all cases, a new final gait is selected; all motions are coupled, and as expected from the

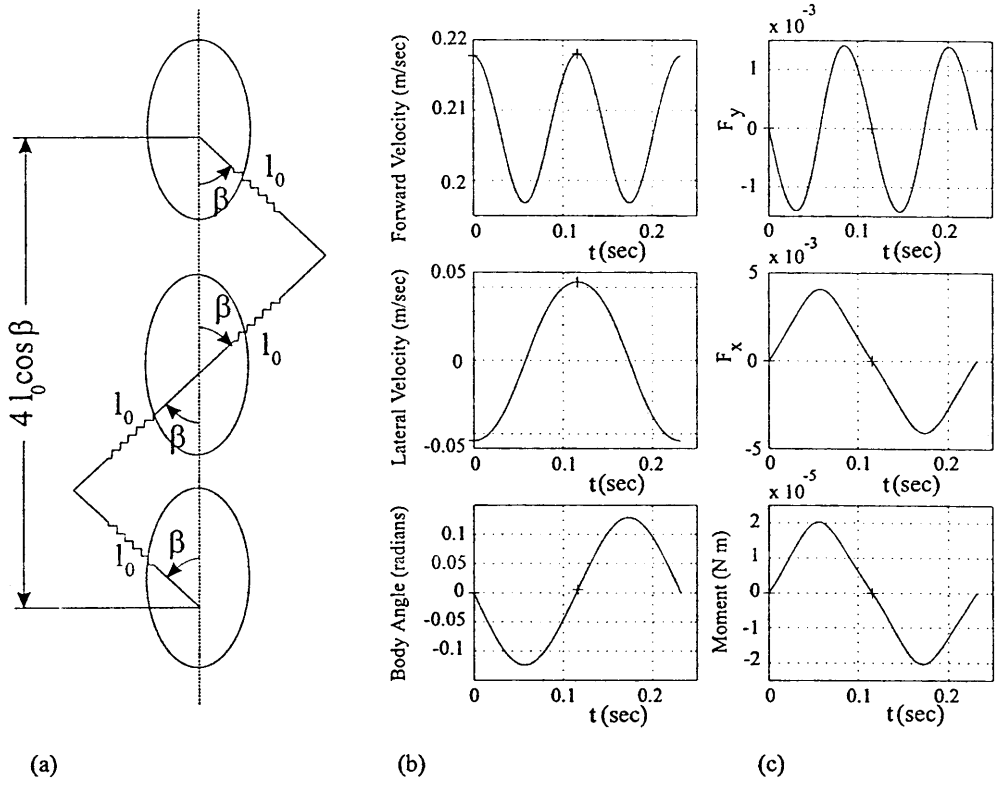

Fig. 2a–c. Characteristics of steady gaits of the fixed centre of pressure (COP) elastic legged system: **a** L-R stride geometry; **b** forward and lateral velocities and angular displacements; **c** fore-aft and lateral forces and torque

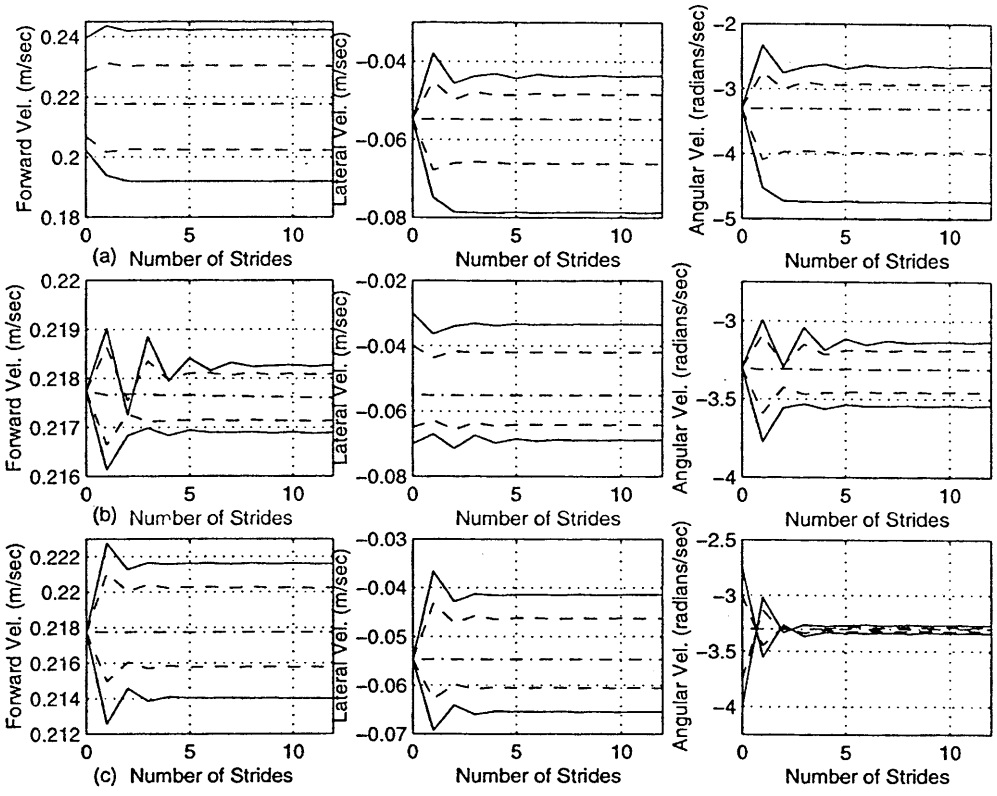

Fig. 3. Linear and angular velocity responses to forward (**a**), lateral (**b**) and angular (**c**) velocity perturbations in the passive spring model. Perturbations shown *solid* and *dashed*; unperturbed gait, *chain dotted*. See text for details

(neutrally stable) unit eigenvalue associated with energy conservation, and from rotational invariance, there is a two-parameter family of gaits that may be characterized by average forward and angular velocity. However, forward velocity perturbations primarily affect only forward velocity, leaving the average orientation unchanged within 1° (Fig. 3a – here the lateral and angular velocity changes reflect selection of a new gait with different heading and orientation variations). Lateral velocity perturbations lead to permanent average heading and orientation changes of up to 6°, (Kubow and Full 1999; Fig. 9) and a concomitant change in $\dot{x}$, the inertial frame velocity shown in Fig. 3b. [Kubow and Full (1999) find recovery to near zero lateral velocity in body coordinates; our results agree with this, since straight running is reestablished at a new orientation; see Fig. 1.] Perturbations in angular velocity also cause the system to seek a new stable gait, but the final angular velocity itself appears insensitive to perturbation size (Fig. 3c).

The recovery rate from perturbations apparent in Fig. 3 matches the larger (slowest) eigenvalue of the linearized full stride map (-0.4699), as one expects for coupled motions (the other eigenvalues are 1 and -0.3853). Note that the eigenvalues are negative, leading to oscillatory decay, illustrated by the plot of forward versus lateral velocity in Fig. 4. Forces generated at the foot or, equivalently, at P, following these perturbations differ by up to 34% in peak values from those of steady running shown in Fig. 2c, but the shapes of the force functions remain similar.

These results differ from those of Kubow and Full (1999), whose model recovered from perturbations in

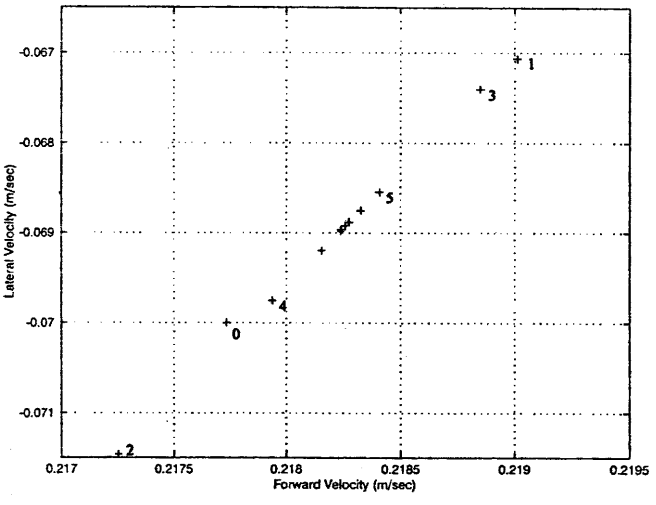

Fig. 4. Recovery from lateral velocity perturbation; orbit of full stride map shown with stride sequence indicated. The nominal fixed point is off-scale at $(0.218, -0.0547)$

each case to the original unperturbed velocities (in body coordinates). We also note that our maximum velocity perturbations are an order of magnitude smaller than the largest used by Kubow and Full (1999) ($\delta\dot{y}$, $\delta\dot{x} = \pm 0.22$, $\delta\dot{\theta} = \pm 30.0$); perturbations of those magnitudes disrupted running irrecoverably, for example by putting the direction of the mass center velocity vector behind the leg direction, so that the body bounces back and cannot proceed. We further discuss our results in comparison with the results of Kubow and Full (1999) in Sect. 3.

2.2 Running with prescribed foot forces

To make possible a more direct comparison with studies of the hexapod model of Kubow and Full (1999), we also considered the bipedal model of Schmitt and Holmes (2000a), Sect. 3.1 with prescribed foot forces which rotate with the body during each stride. The appropriate equations of motion are (1). We took mass and inertia as in Sect. 2.1, and the following foot forces, characteristic of summed tripods, relative to the body frame:

$$\mathbf{f}(t) = [\pm 0.0032 \sin(2\pi t/T_s), -0.004 \sin(4\pi t/T_s)]^T \ , \qquad (5)$$

with full stride period $T_s = 0.1$ s, as in the report of Kubow and Full (1999). Behavior was remarkably sensitive to the touchdown foot position specified via l_0, d and β. For values similar to those of Sect. 2.1, we found stable gaits, with reasonable fore-aft and lateral velocity variations, but with cosinusoidal yaw oscillations of the opposite sign to those observed; this follows, since turning moments about the COM are positive in the first half of each L-stride and negative in the second (and vice versa in R-stride), opposite to those in the animal. For example, with $l_0 = 0.017$ m, $d = -0.001$ and $\beta = 1.25$, we located a periodic gait with average forward speed of 0.211 m s^{-1} and L-touchdown data

$$\bar{v} = 0.224, \ \ \bar{\delta} = 0.143, \ \ \bar{\theta} = -0.057(-3.3^\circ),$$
$$(\bar{\dot{\theta}} = -0.00011) \ ,$$

and forward and lateral velocity oscillations of ± 0.026 and ± 0.039. For $l_0 = 0.017$ m, $d = -0.004$ and $\beta = 1.25$, the forward velocity was significantly slower: $\bar{v} = 0.106$ m s^{-1}.

As noted in (14) of Schmitt and Holmes (2000a), for the special case $\theta(t) \equiv$ constant, there is only neutral velocity stability; recovery to nominal gait following perturbation observed by Kubow and Full (2000a) must therefore be due to coupling with rotation. Indeed, as pointed out there, a jump in forward velocity causes the body to 'outpace' its feet, leading to a turning moment that reorients the body and causes forces during the following stance phase to decelerate it. Similar observations apply to lateral and angular velocity perturbations.

Perturbation results for the first case are shown in Fig. 5 in the same format as in Fig. 3. The unperturbed gait values at L-touchdown were 0.224 m s^{-1} forward, -0.0183 m s^{-1} lateral, and -0.00011 rad s^{-1} angular velocity, and perturbations of similar magnitudes to those in Fig. 3 were used. Since energy is not conserved (see the peg-leg models of Schmitt and Holmes (2000a)), full asymptotic recovery is possible; energy supplied (or removed) by the perturbation is effectively removed (or resupplied) by the prescribed forces, and the open-loop bipedal model shows slow monotonic recovery to the nominal gait following (modest) forward velocity perturbations. Recovery after lateral and angular velocity perturbations is more rapid and oscillatory. The permanent shift in forward and lateral $(\dot{y}, \dot{x})$ velocities in Fig. 5 are due to our use of inertial frame coordinates $(\hat{\mathbf{e}}_x, \hat{\mathbf{e}}_y)$; in body coordinates, the average lateral velocity returns to near zero and straight running resumes. Decay rates are comparable to those of Kubow and Full (1999) (63% recovery in about 80 strides for forward,

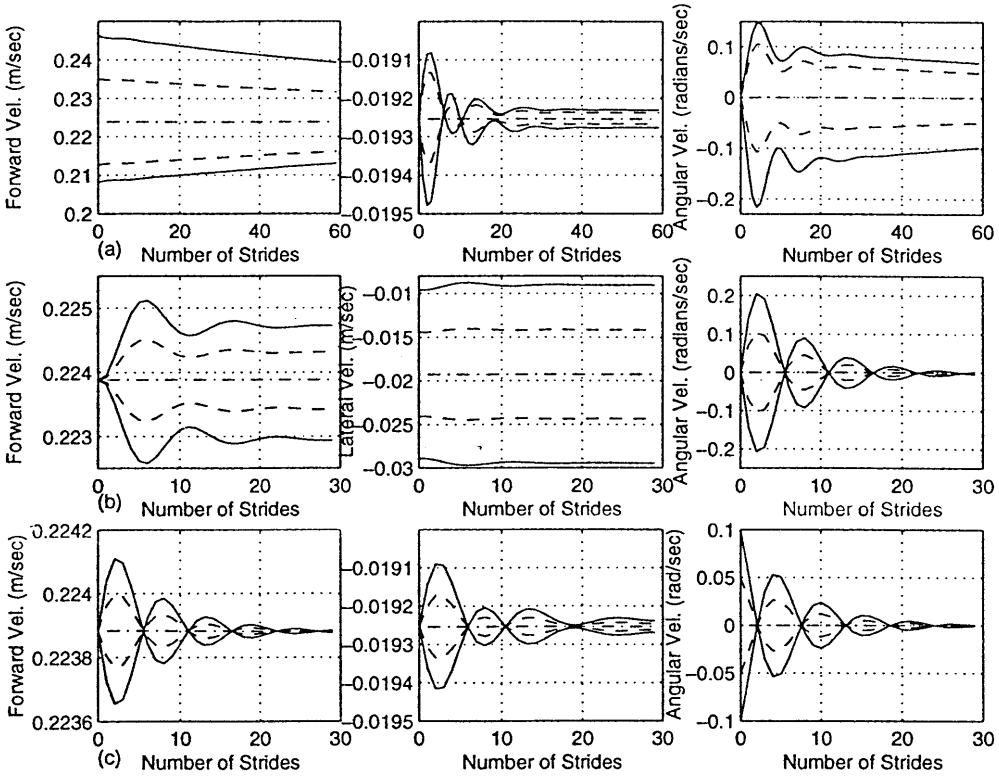

Fig. 5. Linear and angular velocity responses to forward (**a**), lateral (**b**) and angular (**c**) velocities in the prescribed force model. Perturbations shown *solid* and *dashed*; unperturbed gait, *chain dotted*. See text for details

and 8 strides for lateral perturbations, compared to 50 and 8 strides, respectively, in Kubow and Full (1999)). The angular velocity recovers more slowly, in 7 strides; in Kubow and Full (1999), this occurred within one stride. These differences, and the yaw velocity sign discrepancy, are largely due to replacement of the tripod force system with a single virtual leg (Schmitt et al. 2000).

In an attempt to correct the yawing behavior, we significantly decreased the lateral distance to foot touchdown, thus keeping force vector deviations within the triangle defined by foot and COM at touchdown and liftoff. Picking $l_0 = 0.008$ m, $d = -0.0025$ and $\beta = 0.175$ (this small value is necessary to obtain a 'symmetric' stance phase, with COM passing the foot near mid-stance), we obtained qualitatively correct moment and yaw patterns:

$$\bar{v} = 0.228,\ \ \bar{\delta} = 0.088,\ \ \bar{\theta} = 0.0014(0.08^\circ),\ \ (\bar{\dot{\theta}} = 0.0001)\ ,$$

but perturbation studies revealed that this gait was unstable, exhibiting slowly increasing oscillations in response to all perturbations. In this case, moment maxima during L-stance are $\pm 1.3 \times 10^{-6}$ N m, compared with $\pm 7.8 \times 10^{-5}$ N m for the tripod forces of Kubow and Full (1999). While we can match forces reasonably well, moments and yaw amplitudes are significantly smaller, evidently precluding stabilization via yaw coupling. (For the first gait noted above, the moments of $\pm 5.9 \times 10^{-5}$ N m are closer in magnitude to those of Kubow and Full 1999).

In analytical work to be reported elsewhere (Schmitt and Holmes 2000b), we have shown that prescribed forces which do not rotate with the body during each stride always lead to unstable gaits in bipedal models. Since yaw amplitudes are only 1–5°, the rotation matrix $\mathbf{R}(\theta(t))$ in (1) is essentially constant during a stride, and one might expect such a 'minor' change to have little effect. However, this result, and those above, show that stability is a subtle issue for prescribed force models. Although they can display stable behavior, their behavior is fragile and critically dependent upon parameter and protocol choices. In contrast, the compliant-leg models display much more robust stability characteristics.

2.3 Prescribed angle running

Here, we briefly consider a periodic gait with prescribed hip angles, as discussed by Schmitt and Holmes (2000a), and check its stability. An 'impulseless' fixed point of the type described there was found for $\beta = 1.0$ with

$$\bar{v} = 0.2100,\ \ \bar{\delta} = 0.1807,\ \ \bar{\theta} = -0.1133(-6.49^\circ)\ ,$$

and eigenvalues 1, 0.997(≈1) and 0.457. Simulations confirmed stable running and provided the gait characteristics shown in Fig. 6. Body angle variation within a stride is now a negative cosine wave, and forward and lateral velocities exhibit sharp changes in slope (acceleration discontinuities) at touchdown and liftoff, due to

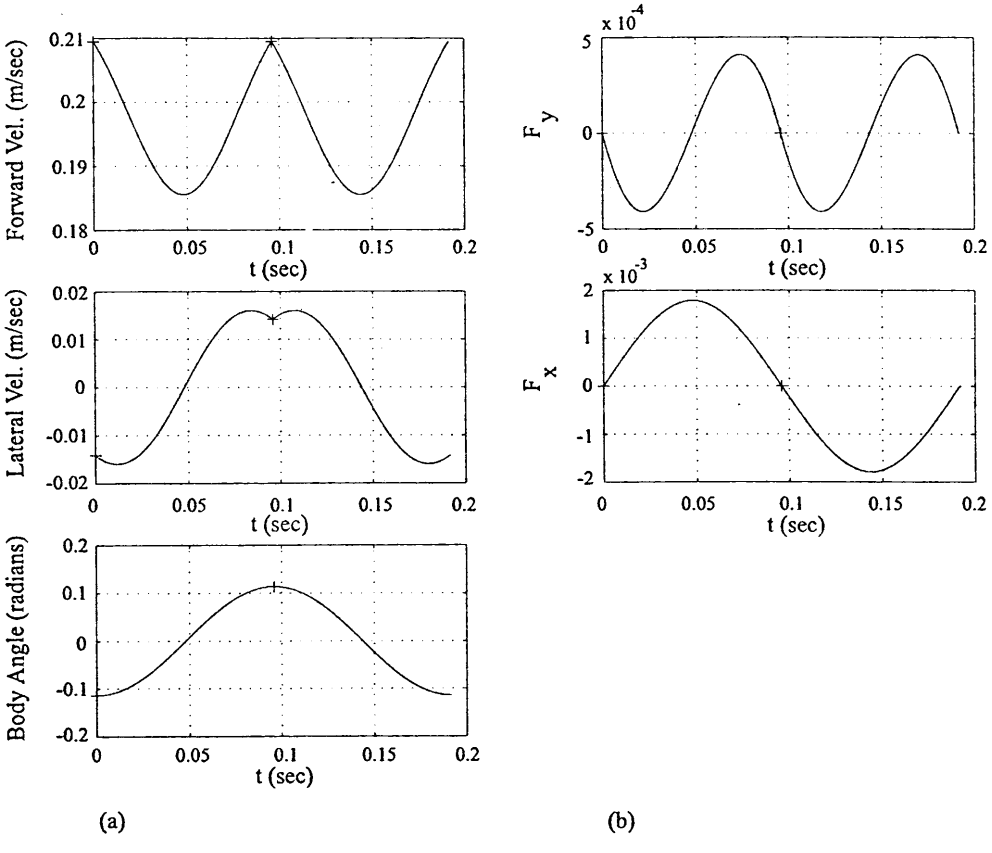

Fig. 6a,b. Characteristics of steady gaits of the prescribed angle model, L-R full stride shown. **a** Forward and lateral velocities and angular displacements; **b** fore-aft and lateral forces

instantaneous imposition of the angular velocity constraint. The force magnitudes are significantly smaller than those observed for the free pivot case (Fig. 2), with consequently smaller variations in forward and lateral velocity during each stride. (Although torques are implicitly applied at P and work is thereby done to maintain the prescribed angles, the forces at the feet, or equivalently at P, determine the full translational dynamics.) Overall, this gait compares poorly with observations; as in the first prescribed force gaits of Sect. 2.2, the applied torques lead to turning moments opposite to those observed, with corresponding negative yaw oscillations.

2.4 Running with moving center of pressure

We simulated the moving COP model of Schmitt and Holmes (2000a), taking m and I as above but with $k = 3.5125$, $l_0 = 0.008$ m, $d_0 = 0$, $d_1 = -0.0035$ and $\beta = 1.125$ (as above, these parameter values were chosen after some trial and error to give an appropriate stride length at the preferred speed). A stable periodic gait was found with

$$\bar{v} = 0.2186, \quad \bar{\delta} = 0.1346, \quad \bar{\theta} = 0.008(0.46^\circ) \ ,$$

and eigenvalues 1, 0.105 and 0.431; Fig. 7 shows the resulting gait characteristics. Fore-aft and lateral velocity and force oscillations are similar in pattern and magnitude to the fixed COP gait (Fig. 2), but the angular variation is now a positive cosinusoid, as in observations. Indeed, d is positive during the first half of each stride and negative in the latter, so oscillating torques are applied during each stride as in the animal itself (Fig. 7b,c).

However, angular variations are much lower than observed, being an order of magnitude below the ± 5–6° reported. Data reduction performed on the hexapedal model of Kubow and Full (1999; Garcia M, personal communication) reveals that the COP and resulting torque time histories are qualitatively similar to those of Fig. 7, but that both are an order of magnitude greater; thus d variations exceed the length of the insect, putting the COP in front of its head and behind its tail at touchdown and liftoff, respectively. We were unable to find stable gaits with d values increased by this order. Evidently, while the single effective leg can represent the summed forces adequately, it cannot successfully reproduce the large torques exerted by the tripod of legs. We are currently studying this in greater detail (Schmitt et al. 2000).

2.5 Strategies for turning

Unlike relatively tall mammals, insects with their splayed postures and low mass centers cannot easily effect turning impulses by 'leaning,' but turns can be achieved by other means. For example, to turn mass

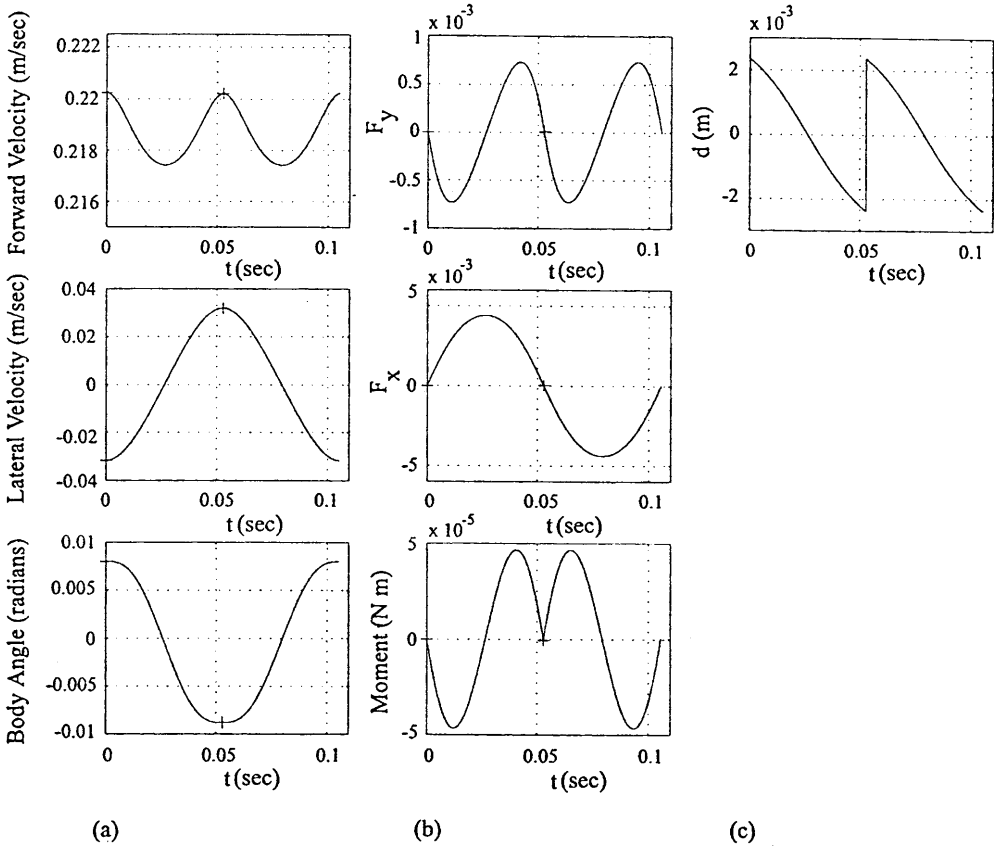

Fig. 7. Characteristics of steady gaits of the moving centre of pressure (COP) elastic legged system, L-R full stride shown. **a** Forward and lateral velocities and angular displacements; **b** fore-aft and lateral forces and torque; **c** COP position

center heading 45° to the left without changing forward speed, impulses of magnitude $mv/\sqrt{2}$ and $mv/(1-1/\sqrt{2})$ must be provided laterally from the right and the front, respectively. In our model, this can be achieved by lengthening and/or stiffening the right leg, possibly also decreasing its touchdown angle β, and shortening/relaxing the left leg, perhaps increasing its touchdown angle. [Recall that stiffness and length are linked in the nondimensional group $\tilde{k} = kl_0^2/mv^2$ of (3).] Increases of β at touchdown increase angular momentum p_ψ, while linear momentum p_ζ decreases; for $d = 0$, this typically increases the angle $\Delta\psi$ swept by the leg, effectively reorienting the mass center heading velocity vector in the desired direction. Decreasing β on the outer leg has a similar effect, via a decrease in $\Delta\psi$.

However, recent experiments reported by Jindrich and Full (1999) suggest that leg angles do not change significantly during turning behavior, whereas leg lengths at touchdown do change. Specifically, the tripod with front and back legs outside the turn appears to generate the bulk of the lateral force and torque necessary to realign both heading and body orientation; the front leg of this tripod is significantly extended on touchdown [by about 11% for turns of $\mathcal{O}(45°)$ accomplished in 1–3 full strides], while the hind leg of the inner tripod is retracted (by about 17%; Jindrich and Full 1999). At liftoff, the inner front and middle legs are significantly shorter (by 19–26%) and the outer hind leg longer (by about 20%). Length changes are presumably achieved by varying the 'horizontal posture' (joint angles). The strategy described below therefore primarily uses adjustable leg length and stiffness, the effects of which our model combines in $\tilde{k}$. In fact, we expect that larger joint angles corresponding to increased leg lengths might also confer increased stiffness in the insect, and vice versa.

In the following descriptions, although turning continues after nominal parameter values are restored, we refer to the stance periods during which parameter changes are in effect as the turn steps. After several strides of steady straight motion, starting on the right (R) touchdown, we changed kl_0^2 by factors of up to 2 (or 0.5) on the R (or L) legs, sometimes accompanied by changes in β by up to 0.8 (or 1.25 for L), for 2–6 steps. After the turn steps, all parameters reverted to their nominal 'straight running' values. With nominal $\beta = \pi/4$ (for which the admissible range of touchdown heading angles δ is relatively narrow), the larger changes frequently led to 'crashes' in which the mass center heading angle at touchdown fell outside the allowable range. When this did not occur, turns were generally modest (0–5°) and sometimes to the right, the direction opposite to that desired (see Fig. 8a for a representative example using $\beta = 1.0$). This behavior follows from the fact that, with $d < 0$, the torque impulse occurs in the direction opposite to the desired turn, since the increased R leg force produces a clockwise torque. Orientation subsequently overcorrects and the asymptotic stability of orientation/heading coupling eventually settles the body on its new course. The out-of-phase patterns of orientation and heading evolution through the turn shown in Fig. 9a differ markedly from the small [$\mathcal{O}(5°)$] differences observed by Jindrich and Full (1999; Table 1 and Fig. 4E). In terms of that paper, the 'leg effectiveness' is poor; a desired linear momentum change to change heading is accompanied by an undesired angular

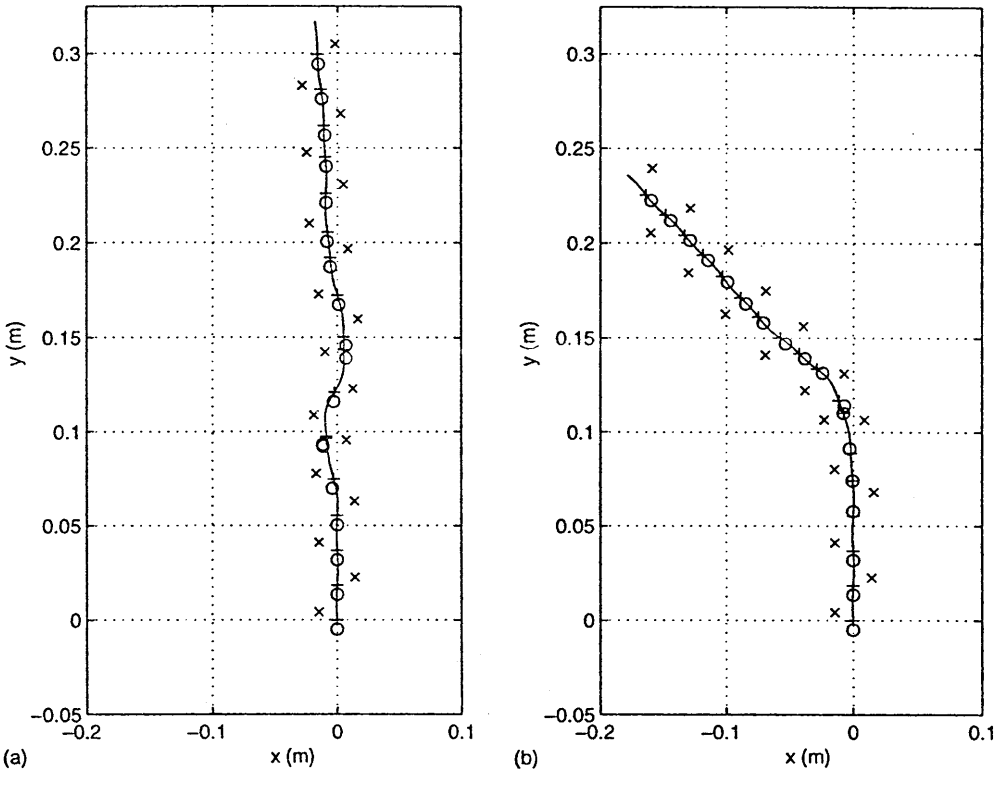

Fig. 8. Turning behaviors with COP fixed (**a**), and varied (**b**); nominal parameter values as in Sect. 2.1, but with $\beta = 1$; turn started on fourth step: (a) kl_0^2 changed by factor of 2 (or 0.5) and β by 0.833 (or 1.2) on three consecutive steps R-L-R; (b) kl_0^2 changed by factor of 1.5 (or 0.667) on four consecutive steps R-L-R-L, $\beta \equiv 1$, $d = +0.0025$ on R; $d = 0$ on L during turn steps

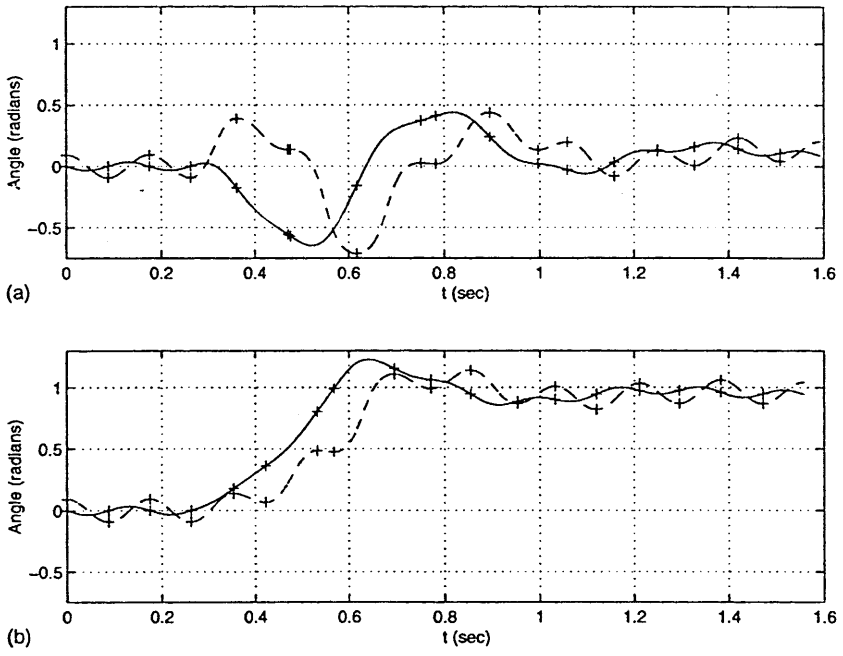

Fig. 9. Body orientation θ (*solid*) and mass center heading angle $-\arctan(\dot{x}/\dot{y})$ (*dashes*) through the turns of Fig. 8a and b; $+$'s indicate touchdown/liftoff instants

momentum change, negatively affecting orientation. Larger ($\mathcal{O}(45°)$) turns could be obtained by careful choice of initial data, but they were non-robust and involved unrealistically short steps ('stumbles') and large impulses.

We therefore decided to allow changes in d, with a view to modeling the effect of the insect 'favoring' its outside front leg during the turn while deemphasising its inside hind leg, consistent with the observations of Jindrich and Full (1999) summarized above. We set $d > 0$ on R leg stance, and $d \approx 0$ on L leg stance during the turn steps. Stable turns of 20–70° were then easily elicited in 2–6 steps, with changes in kl_0^2 of order 2 (or 0.5), both with and without changes in β. Turns were also obtained with no change in kl_0^2 or β. Figures 8b–9b show a representative example, again with $\beta = 1$. On shifting the COP, the unstable behavior associated with $d > 0$ helps produce the required reorientation (no change in β is needed), but some overshoot of orientation occurs, and several steps following the turn steps are required to achieve and stabilize the new heading. Most of the turn is accomplished over 3–5 steps in a 250–450-ms period, during which heading lags orientation by 5–15°, and there is considerable variability in stance period. Throughout, heading fluctuations are generally greater than those of orientation. These results are in reasonable agreement with observations, although in Jindrich and Full (1999), it was found that heading led orientation by 5° on average (with considerable variability among both animals and trials). This difference is perhaps related to the 'unphysical' yawing behavior of the fixed COP model during steady running (see Sect. 2.1 and Fig. 2a).

Left turns were more easily accomplished, and larger angle changes obtained, starting with an R-turn step. This can be understood by considering body angular velocity, which is positive in straight running at R touchdown, so that body orientation is already moving in the appropriate direction (Fig. 9b). Left turns initiated by L-turn steps were possible, but displayed body orientations opposite to the desired direction early in the turn. We computed foot forces throughout the turns and checked that integrated foot impulses matched the linear momentum changes observed.

Preliminary simulations of turning for the moving COP model gave very similar results to those of Figs. 8b–9b. Turns of 40–75° were easily achieved in 2–5 steps simply by transiently biasing the COP position forward on the outer leg. For a left turn, this was achieved by setting $d_0 = 0.0025$ on two succeeding R steps, while otherwise keeping $d_0 = 0$ throughout. This effectively increases the leg length at touchdown (the pivot being further forward), and keeps the pivot ahead of the COM for most of the stride, thus biasing the moment arm to produce the desired torque and reorientation. Force magnitudes increased by up to 70% during the turn, and no changes in l_0, β or k were necessary. Detailed studies will be published elsewhere Schmitt and Holmes (2000b).

We note that, during 'emergency' behaviors such as wedging and self righting, cockroaches can produce leg forces an order of magnitude greater than those used in normal running (Full and Ahn 1995; Full et al. 1995); the relatively modest transient force increases required above are thus quite reasonable.

3 Conclusions and future work

In this and the preceeding paper (Schmitt and Holmes 2000a), we have developed and analysed models for legged insect locomotion in which the tripod support stance phases are replaced by a single 'virtual' compliant leg, and angular momentum is conserved about the current 'foot' position in each such phase, with instan-

taneous switches at touchdown/liftoff (no double stance phases). We consider dynamics only in the horizontal plane. Our models are rigid bodies, representing the head-thorax-abdomen, free to translate and rotate on a frictionless plane, subject to intermittent constraints due to foot placement.

With a fixed 'hip' (or coxa-body) pivot P and virtual legs attached at P behind the mass center, we find energy-conserving periodic gaits that display (strong) asymptotic stability with respect to heading and body orientation, and that share many features of gaits observed in the death-head cockroach *Blaberus discoidalis*. When angular leg displacements are prescribed relative to body orientation, we also find that stable gaits are possible, although we have only investigated a limited class of motions which do not suffer angular impulses at touchdown. These fixed COP and prescribed angle models can be seen as limiting cases; neither yields correctly phased yawing motions, and a more realistic model would probably fall between these two extremes. The moving COP model, which also displays stable gaits, goes some way in this direction, but is unable to produce yawing motions of sufficient size.

Our models are simple and idealized; in particular, we neglect frictional and other losses (due to muscles, for example). Including such losses, with a suitable energy input, perhaps due to applied torques at P, we expect to obtain equilibration and asymptotic stability of forward velocity; endowing the legs with mass and inertia would also lead to energy losses due to impact on touchdown. Even in our simplified model, there are four parameter groups; nondimensional stiffness $\tilde{k}$ (or $\tilde{c}$), inertia $\tilde{I}$, 'hip distance' $\tilde{d}$, and touchdown angle β (3). We can estimate values (for *Blaberus discoidalis*) from the measurements of Full et al. (1999), but our parameter studies have been limited. Taking $\beta = \pi/4$ and $l_0 = 0.017$ m, we obtain a gait with velocity, angle and force oscillations comparable to those observed, but with relatively slow, long strides; $\beta = 1$ and/or $l_0 = 0.01$ m give more realistic stride frequencies, but gait variations are then too small. This may be an effect of our replacement of the support tripod by a single leg; reduction to a single virtual leg certainly reduces torque and hence yawing magnitudes in the moving COP case. Further examination of gait dependence on parameters is needed, as has been done for saggital plane models (Blickhan 1989; McMahon and Cheng 1990) and this is currently in progress (Schmitt and Holmes 2000b). Nonetheless, a general predicition emerges; a rearward shift of the mass center should promote instability. It would be interesting to test this on 'prepared' insects.

We may also essay a tentative comparison of our findings with those of Kubow and Full (1999), who studied the response of a rigid body moving under prescribed force components applied at foot locations and with magnitudes derived from observations of steady straight running of *Blaberus*. Perturbations of forward, lateral and angular velocity $(0.22 \pm 0.22\ \mathrm{m\ s^{-1}})$, $(0 \pm 0.20\ \mathrm{m\ s^{-1}})$, and $(0 \pm 30\ \mathrm{rad\ s^{-1}})$, respectively, were applied at the beginning of a stance phase. Forward velocity recovered to its original value slowly (63% recovery in about 50 strides), lateral velocity recovered more rapidly (63% in about 8 strides) with a permanent change in heading direction, and angular velocity recovered within one stride (see Kubow and Full 1999; Figs. 5–14 and accompanying text). However, forces were not allowed to respond to perturbations, a questionable assumption, particularly in view of the fact that for large forward and lateral velocity perturbations, the body may move outside the 'straight running' support tripod assumed by the model. Presumably, large leg displacements resulting from large perturbations would significantly modify force magnitudes and directions, and feet could skid or lose contact entirely. (We find force magnitudes in compliant legs change by up to 34% for significantly smaller perturbations than those of Kubow and Full 1999).

One qualitative similarity between the behavior of our free pivot model and these results is the emergence of three timescales from the three eigenvalues $\lambda_1 = 1$, associated with forward velocity, and $|\lambda_3| (\approx 0.39) < |\lambda_2| (\approx 0.47)$, associated with heading direction and body angular velocity, obtained for $d < 0$ [Sect. 3.2–3.4 of Schmitt and Holmes (2000a) and Sect. 2.1 above]. We do not see a clear separation of time scales, nor the near-instantaneous recovery from angular velocity perturbations (Kubow and Full 1999; Fig. 14a). However, our observation of relatively rapid recovery in orientation and lateral velocity (in the body frame) does agree with the general picture presented in Kubow and Full (1999); we find 63% recovery from lateral and angular perturbations in about 5 strides. On the addition of weak (frictional or impact) dissipation, we would expect our neutral stability to forward velocity perturbations ($\lambda_1 = 1$) to become weak asymptotic stability, comparable to the slow (50-stride) recovery. We cannot expect close agreement, since Kubow and Full (1999) essentially solve an 'open loop' problem, with fixed force histories applied in a periodic clock-driven manner, while our compliant-legged 'closed-loop' models generate forces depending upon body motions, and liftoffs and touchdowns are event-driven. Applying prescribed forces to the bipedal model, we can obtain stable gaits as in Kubow and Full (1999), albeit with reversed yaw oscillations; on correcting the sign, yawing torques are up to 60-times smaller than those for the hexapod, and gaits are unstable. (Disallowing forces to rotate with the body during a stride also results in unstable gaits; Schmitt and Holmes 2000b). Overall, we find the 'robust' mechanical feedback of the compliant leg models more plausible in accounting for gait stability than carefully chosen open-loop prescribed forces.

Our studies of turning are only preliminary, but we have shown that the free pivot, fixed and moving COP models can effect stable turns of 20–75° in 2–6 steps by transiently varying touchdown angles, leg lengths and compliances, along with a forward shift of the attachment point (COP) P. The shift of P is essential (and sufficient alone) to elicit turning; (small) turns are possible with fixed $d < 0$, but they are fragile – parameters must be selected carefully to avoid unstable behavior – and the resulting body orientation and heading behaviors

are unnatural. Our strategy of shifting P seems plausible in that it might capture the differing 'leg effectiveness numbers' identified by Jindrich and Full (1999), but an examination of hexapedal models may be needed to properly understand turning (the final frame – step 5 – of Fig. 8A of Jindrich and Full (1999), for example, shows a lateral force impulse directed to the left while the L-tripod is down; this is impossible for our biped). We find the use of natural (unstable, $d > 0$) dynamics and nonzero yaw velocities to achieve body reorientation appealing, but we recognize that the precise way in which yawing during steady running 'feeds into' turning probably differs from that in free pivot models. However, again a qualitative prediction emerges; if passive dynamics is implicated in turn stabilization, then neural 'turn signals' leading to stance changes should be detected only during the early part of a turn (Figs. 8b, 9b).

Although much of the theory developed by Schmitt and Holmes (2000a) applies to general spring laws, we have focused on the linear spring for specific calculations and for the simulations above. At this stage, seeking general properties, we did not think it wise to attempt a detailed model of individual limbs or muscles (see Full and Ahn 1995). The linear spring has the advantage of simplicity and explicit solubility (for $d = 0$), with the disadvantage of non-physical behavior at high velocities. However, in this respect, the requirement that the non-dimensional parameter $\tilde{k} = kl_0^2/mv^2 > 1$ for physically acceptable behavior (see discussion following (33) of Schmitt and Holmes 2000a) is not as stringent as might appear, since it is reasonable to suppose that, in insects, the effective leg stiffness can be adjusted to 'match' different forward speeds. We are currently investigating this (Schmitt et al. 2000), in an attempt to model the stride length and frequency variations reported by Ting et al. (1994).

In addition to the parameter studies mentioned above, to bring our models closer to reality, in future work we plan to include double stance phases (duty factor $> 50\%$) and, in an attempt to move towards multiple legs and tripod support, to further study moving COP models. The former will disrupt conservation of angular momentum, since there are now two attachment points. The latter will require a proper understanding of under what conditions, and how, multiple legs can be 'collapsed' to a single equivalent (nonlinear) spring; this may be particularly important for understanding turning behavior. We also wish to include compliant torsional springs at the attachment point(s) P, to add finite leg masses and inertias, and to consider frictional and other losses and their effects on asymptotic stability and forward speed selection. We believe that, while retaining the (relative) simplicity of a single effective leg for each tripod, such extensions of the basic models developed here can give further insight into the stability and control of insect running.

Acknowledgements. This work was begun at the Institute for Mathematics and its Applications Workshop on Animal Locomotion and Robotics in June 1998, and was thereafter supported by DoE: DE-FG02-95ER25238 and DARPA/ONR: N00014-98-1-0747. John Schmitt was partially supported by a DoD Graduate Fellowship and a Wu Fellowship of the School of Engineering and Applied Science, Princeton University. We thank Mike Coleman, Bob Full, Mariano Garcia, Devin Jindrich, Dan Koditschek, Tim Kubow, and Andy Ruina for numerous comments, corrections, and suggestions.

References

Blickhan R (1989) The spring-mass model for running and hopping. J Biomech 11/12: 1217–1227

Full RJ, Tu MS (1990) Mechanics of six-legged runners. J Exp Biol 148: 129–146

Full RJ, Tu MS (1991) Mechanics of a rapid running insect: two-, four- and six-legged locomotion. J Exp Biol 156: 215–231

Full RJ, Ahn AN (1995) Static forces and moments generated in the insect leg: comparison of a three-dimensional musculoskeletal computer model with experimental measurements. J Exp Biol 198: 1285–1298

Full RJ, Yamauchi A, Jindrich DL (1995) Maximum single leg force production: cockroaches righting on photoelastic gelatin. J Exp Biol 198: 2441–2452

Jindrich D, Full RJ (1999) Many-legged maneuverability: dynamics of turning in hexapods. J Exp Biol 202: 1603–1623

Kram R, Wong B, Full RJ (1997) Three-dimensional kinematics and limb kinetic energy of running cockroaches. J Exp Biol 200: 1919–1929

Kubow TM, Full RJ (1999) The role of the mechanical system in control: a hypothesis of self-stabilization in hexapedal runners. Phil Trans R Soc Lond B 354: 849–861

McMahon TA, Cheng GC (1990) The mechanics of running: how does stiffness couple with speed? J Biomech 23: 65–78

Schmitt J, Holmes P (2000a) Mechanical models for insect locomotion: Dynamics and stability in the horizontal plane – theory. Biol Cybern 83: 501–515

Schmitt J, Holmes P (2000b) Mechanical models for insect locomotion: Perturbation, stability and parameter studies. Physica D (in review)

Schmitt J, Holmes P, Full RJ, Garcia M, Razo R (2000) Dynamics and stability of legged locomotion in the horizontal plane: A test case using insects. Preprint, Dept of Mechanical and Aerospace Engineering, Princeton University

Ting LH, Blickhan R, Full RJ (1994) Dynamic and static stability in hexapedal runners. J Exp Biol 197: 251–269